Seismic Sensor Network for High Density Deployments: Concept, Design, Deployment and Results

Marco Manso[1](✉) , Mourad Bezzeghoud[1,2], José Borges[1,2], and Bento Caldeira[1,2]

[1] Instituto de Ciências da Terra, Universidade de Évora, Évora, Portugal
marco@marcomanso.com
[2] Departamento de Física (ECT), Instituto de Ciências da Terra (IIFA), Universidade de Évora, Évora, Portugal

Abstract. The devastating impact that seismic events can cause to societies demands that the underlying physical processes that cause them are better understood. Seismic networks have been increasingly deployed over the years allowing to measure ground motion with great accuracy and, in a few cases, reaching high-density deployments for high-resolution measurements. In this chapter it is described the work conducted to build a high-density seismic network comprised of low-cost network-enabled accelerometer sensors to monitor the Alentejo region. The design resulted in a modular platform that can operate with different sensors. Following a noise performance evaluation, the Analog ADXL355 accelerometer was selected for the deployment phase. Herein, sensor system measurements were compared with a professional seismometer, using two actual seismic events recorded in Portugal. These events allowed to demonstrate the sensors capabilities in detecting weak (2.5 ML) to moderate (3.4 ML) seismic events at short (8 km) and medium (140 km) distances respectively. Comparing obtained measurements with a professional seismometer, however, the sensor prototypes exhibited, as expected, a higher presence of sensor noise. Overall it is concluded that the sensor system has a potential application in seismology.

Keywords: High-Density Seismic Network · Seismic Sensors · MEMS · Accelerometers · Seismology · Sensor noise

1 Introduction

Seismic events can be extreme and severely threat whole societies, causing a high death toll, victims and property damage. Taking as a recent example, the 2004 Sumatra Earthquake and Tsunami in Indian Ocean started with an undersea earthquake with a magnitude of 9.1, generating a tsunami that devastated "coastal areas as far away as East Africa. […] The tsunami killed at least 225,000 people across a dozen countries, with Indonesia, Sri Lanka, India, Maldives, and Thailand sustaining massive damage." [1] The Iberian Peninsula and the North of Africa - part of the Ibero-Maghrebian region between the Gulf of Cadiz and Algeria – also register the occurrence of large earthquakes

since they share the Eurasian–Nubian plate boundary that corresponds to a well-defined narrow band of seismicity [2].

Helping to understand the physical processes that cause earthquakes, seismic networks, capable to measure ground motion in great accuracy, have been deployed in increasing number. Portugal, in particular, has made a significant effort to develop the Broadband Portuguese seismic network integrating seismological stations from various institutions supporting real-time monitoring of the earthquake activity [3, 4]. Between 2010 and 2012, the West Iberia Lithosphere and Asthenosphere Structure (WILAS) project integrated a temporary network of 20 sensors in the Portuguese national network resulting in a total of 55 stations spaced on average by 50 km [5, 6]. These stations continuously recorded measurements at frequencies up to 100 Hz, thus collecting a large volume of high-quality data of densely distributed broadband stations [7]. More recently, the Arraiolos seismic network (in Alentejo) was deployed comprising 14 broadband stations (CMG 6TD, 30s) of the Institute of Earth Sciences of Évora, Portugal (Instituto de Ciências da Terra or ICT) and temporarily extended with 21 short-period stations (CDJ, 2.0 Hz) of the Dom Luiz Institute of Lisbon, Portugal (Instituto Dom Luiz or IDL) within a 20 km radius [4, 8].

In the continued endeavor to increase seismic monitoring resolution by deploying more seismic stations, researcher have exploited recent technological innovations applied to sensors and sensor platforms covering increased performance, reduced energy consumption, improved connectivity, miniaturization and reduced cost. Combined together, these innovations enable the deployment of large sensor networks for "live" (online and real-time) monitoring of seismic activity with high spatial resolution [9], as well as with the potential to identify precursor signals associated with earthquakes [10], a capability that can be used for Early-Warning applications and thus to alert populations and reduce the time to respond to a disaster. It is herein presented a few cases of high-density seismic sensor deployments:

a) **Sensor Network deployed in the Long Beach Area:** During 2011, more than 5200 high-frequency (10-Hz corner frequency) velocity sensors, with an average spacing close to 100m, were deployed in the Long Beach area as part of a petroleum industry survey [11]. The main purpose was to better define the area, including construction of a high-resolution 3D shallow crustal structure. The Long Beach high-density deployment was a pioneering effort that demonstrated the high-resolution observation and reconstruction of seismic activity.

b) **University of Southern California's (USC) Quake-Catcher Network (QCN):** is a seismic network that implements distributed/volunteer computing with the potential to provide critical earthquake information by filling in the gaps between traditional seismic stations [12]. Initially, it started to exploit data produced by accelerometers pre-installed in computers and now uses USB-connected Microelectromechanical systems (MEMS) accelerometers and mobile-phone accelerometers. The system communicates via the Berkeley Open Infrastructure for Network Computing (BOINC) [13]. QCN can only record strong motion and requires a connected computer to operate.

c) **CalTech's Community Seismic Network (CSN):** established by 2009, consists in an earthquake monitoring system based on a dense array of low-cost acceleration sensors aiming to produce block-by-block measurements of strong shaking during an earthquake[1]. In 2015, CSN was described as a 500 element network located in the Los Angeles area of California in the USA [14]. The expansion plan throughout the Los Angeles region consists in deploying sensors in schools by involving the Los Angeles Unified School District (LAUSD). The expansion started with 100 schools and was later supplemented with additional 200 campuses. The plan is to reach all 1000 campuses of LAUSD and extend to other public and private schools in the region (4000 campuses in total).

d) **MyShake Platform: Leveraging on Mobile Phones:** The MyShake Platform is an operational framework to provide earthquake early warning (EEW) to people in earthquake-prone regions. It is built on existing smartphone technology to detect earthquakes and issue warnings [15]. Over 300,000 people around the globe have downloaded the MyShake app, however the number of active users (i.e., active phones connected) only peaked at 25k.

e) **SSN Alentejo:** The Seismic Sensor Network Alentejo (SSN-Alentejo) developed by ICT brings the most dense seismic sensor network ever deployed in Portugal. This novel network aims to improve the characterization of seismic activity in the region and to improve earthquakes' assessment. Planned for 2020 and 2021, SSN-Alentejo will deploy a monitoring network of 60 sensors to generate significant volumes of live data and advance seismology knowledge. The sensors will be distributed in a mesh configuration spaced on average 10 km and covering an area of about 5000 square kilometers.

The evolution of the seismic network in Arraiolos and planned deployments for SSN-Alentejo are presented in Fig. 1 [16].

The remainder of this chapter is organized as follows: Sect. 2 presents the potential application of MEMS accelerometers for seismology, including their advantages and limitations; Sect. 3 describes the sensor system designed and built for seismological applications, incorporating MEMS accelerometers and network-enabled capability. The section also describes work conducted to evaluate the noise present in several MEMS accelerometers, while measuring at rest, which allows to identify the most appropriate accelerometers for seismic operations. Importantly, the developed method can also be applied on-site and in-operation, to determine the occurrence of seismic events. Section 4 present results of deploying and testing a MEMS sensor system (defined in Sect. 3) with the ADXL355 accelerometer, including results obtain from two recorded seismic events in Portugal, using a reference seismic station for comparison purposes. Section 5 presents the main conclusions of the paper, also outlining future possible work.
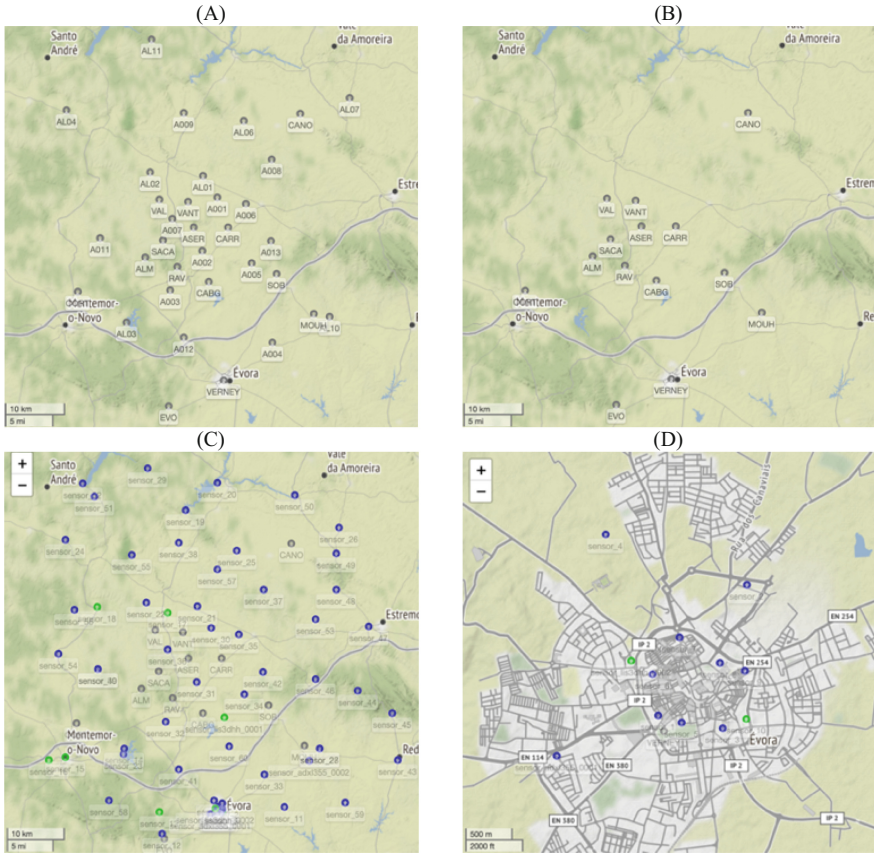
---

[1] http://csn.caltech.edu.

Fig. 1. Different phases of the seismic network in Alentejo (includes the Arraiolos region) and the SSN-Alentejo planned deployment. (A) Temporary seismic network deployed in the Arraiolos region after the earthquake. About 60 connected stations. (B) Current seismic network in the Arraiolos region. Less than 15 connected stations. (C) SSN-Alentejo: planned deployment of additional 60 sensors, resulting in about 75 stations in total. (D) SSN-Alentejo: planned deployment for the Évora city. Sensor density is increased to monitor ground motion activity that may impact cultural heritage and historical buildings [16]. The SSN-Alentejo project is funded by the Science Foundation of Portugal (FCT) under grant number ALT20–03-0145-FEDER-031260.

2   MEMS Accelerometers for Seismology

The evolution in sensors and sensing network technology has brought improvements in performance (resolution, sensibility and processing capacity), operation (energy efficiency, operation time) and connectivity (broadband communications), at a significant cost reduction [17]. Low-cost MEMS accelerometers, in particular, demonstrated the capability to generate relevant data for seismic analysis in dense deployment contexts [18]. MEMS technology has enabled the mass production of small size accelerometers. Capacitive accelerometers, in particular, are highly popular due to reduced cost, their simple structure, and the ability to integrate the sensor close to the readout electronics.

When subjected to an acceleration, the inertial mass shifts cause a proportional change in capacitance. By measuring the capacitance change, the acceleration can be calculated.

For purposes of seismology and as presented by Manso *et al.* [9], state-of-the-art low-cost MEM-based accelerometers:

a) provide adequate sensitivity, noise level, and range (measured in g) to be applicable to earthquake strong-motion acquisition (M > 3.0), thus also limiting the "resolution" capability. However, the high level of instrumental self-noise that increases as frequency decreases limits their application in the study of low frequency weak-motion forces [19, 20];

b) are well fit to measure high frequency (>40 Hz) ground motion [20] since their resonant frequency (typically above 1 kHz) is far above the seismic band pass;

c) measure the gravity acceleration component that provides a useful reference for sensitivity calibration and tilt measurement;

d) have high acceleration ranges (several g) and are capable to sustain high acceleration (several hundred g) without being damaged;

e) when compared with seismometers, such as geophones, may have an advantage in detecting weak high frequency signals, while geophones may have the advantage in detecting weak signals at low frequencies;

f) can have useful applications such as Earthquake Early Warning System (EEWS), seismic hazard map and security applications [21].

As the underlying technologies to build connected MEMS systems became more accessible and affordable, several efforts are currently using dedicated MEMS sensors to build dense seismic sensor networks, as the case of CSN and the urban MEMS seismic network in the Acireale Municipality (Sicily, Italy) [22]. They have found several fields of application, including: seismological study and earthquake observation, seismic activity monitoring networks, and seismic surveys [23].

3-axis MEMs accelerometers are already used to augment existing seismic networks, essentially filling in the gaps between higher-quality sensors [24]. Furthermore, MEM technology will surely continue to evolve and it is expected that their performance on weak low frequency signals will improve.

3   The Network-Enabled Seismic Sensor System

Presented in [25], the authors developed a prototype for a seismic system using a MEMS accelerometer connected to a microcontroller. The system operates autonomously, is network enabled and is capable to deliver high data throughput. The sensor system is presented next. Note that three different sensors were used for evaluation purposes (Table 1).

Table 1. Seismic sensor system architecture components.

Component	Architecture component see [25]
ESP8266	Acquisition and processing board (32-bit processor at 80 MHz); Storage (internal flash, between 512 KiB and 16 MiB); Networking (integrated TCP/IP protocol stack, Wi-Fi)
TDK InvenSense MPU-6050 or ST LIS3DHH or Analog ADXL355	MEMS accelerometer
Internal clock synchronised with NTP	Real-time clock

For the Acquisition and Processing Board, the ESP8266 is selected because it provides: a fast and programmable microcontroller (operates at 80 or 160 MHz); Storage capabilities (embedded flash up to 4 MiB); Networking capabilities (via its embedded Wi-Fi chip). RTC time synchronisation is achieved by means of Network Time Protocol (provided by a NTP server). The ESP8266 also supports a wide range of libraries, in large part provided by the Arduino community.

Concerning the accelerometer, three different components were integrated: MPU-6050, LIS3DHH and ADXL355.

The sensor system overview including components' interconnections are presented in Fig. 2. The pin connections between the components are presented in figure. Note that the depicted accelerometer is the MPU-6050. The data interface used is the I2C Digital Interface (Table 2).
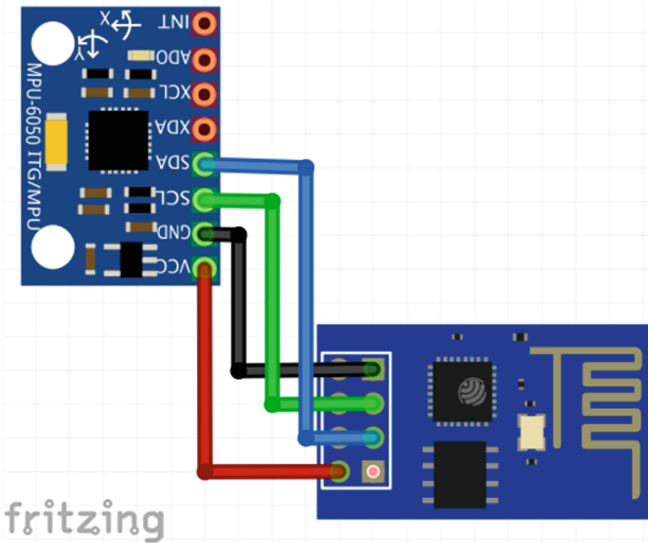

Fig. 2. Sensor system interconnections [25].

Table 2. Sensor system interfaces [25].

Interface	ESP Pin	Sensor Pin
I2C	Pin 0	SDA
I2C	Pin 2	SCL

The sensor system was designed to rely in existing network and power infrastructure. In this regard, the design did not seek power consumption optimisation.

3.1   Noise Performance Comparison

Section 2 introduced MEMS accelerometers, describing their application for seismology, also mentioning as a main limitation the presence of sensor noise that is originated from the sensor's electrical and mechanical components. In this subsection, an indication of sensor noise, first described in [17], is measured by deploying and collecting acceleration data, while at rest position, from the different sensors used in the sensor system.

The sensor noise assessment is made by calculating the standard deviation of the signal (calculated using a "moving window" of 100 samples). The lower the standard deviation the lower the sensor noise.

The standard deviation is calculated using the well know formula 1:

$$\sigma = \sqrt{\frac{\sum (x_i - \mu)^2}{N}} \qquad (1)$$

where:
i is the sample number,
x_i is the measurement related with sample i,
μ is the mean value and.
N is the sample size.

The environment where accelerometers are installed might be affected by external factors (e.g., traffic or seismic activity), which can be registered by accelerometers and should be excluded from the sensor noise analysis. In order to exclude these "signals" from "noise", a threshold logic is defined and implemented as follows:

```
let σ(n) be the standard deviation related with sample window n
let σ_min be the registered minimum standard deviation for the running
   period

if ( σ(n) > σ_min . Threshold ) then
   is signal
else
   is noise
endif
```

The following devices were analysed:

- A TCL mobile phone
- A Xiaomi mobile phone
- A CAT mobile phone
- TDK InvenSense MPU-6050 (used in the sensor system)
- ST LIS3DHH (used in the sensor system)
- Analog ADXL-355 (used in the sensor system)
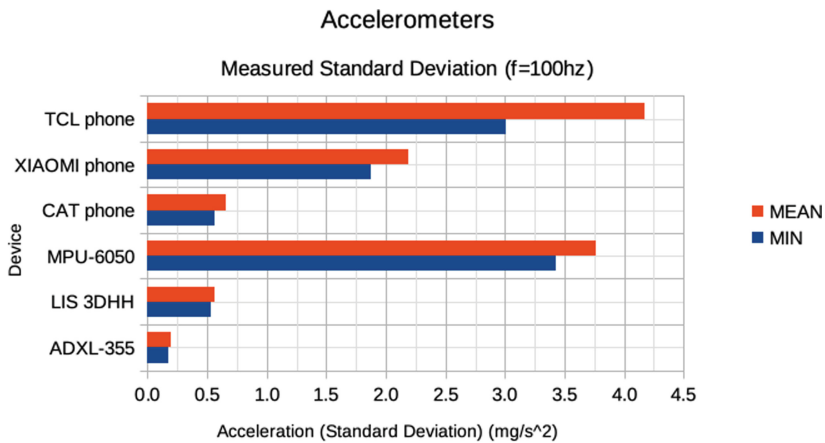
The results are presented next.

Fig. 3. Measured standard deviation for several accelerometers operating at a sampling rate of 100 Hz [17].

Table 3. Measured standard deviation for several devices: minimum recorded value and mean value [17].

Device	σ_{MIN} (mg)	σ_{MEAN} (mg)
TCL phone	3.0115	4.1707
XIAOMI phone	1.8716	2.1893
CAT phone	0.5595	0.6563
MPU-6050	3.4253	3.7606
LIS 3DHH	0.5270	0.5634
ADXL-355	0.1734	0.1950

The developed method yields an indication of sensor noise, which is sensor specific. As shown in Fig. 3 and Table 3, the dedicated accelerometer ADXL-355 yields the lowest minimum standard deviation (0.1734 mg), followed by the LIS 3DHH (0.5270 mg), the CAT phone (0.5595 mg). The TCL phone and the MPU-6050 yield the highest values,

with 3.0115 mg and 3.4253 mg respectively. It is also pertinent to note the disparity between the mean and the minimum value of standard deviation for the TCL phone, indicating that the minimum value for standard deviation alone is not sufficiently robust to assess sensor noise in actual deployments.

The presented analysis of sensor noise observed in different types of accelerometers, successfully developing a method to measure noise on-site and in-operation. The method produces an indication of sensor noise based on the measured standard deviation. It yields results consistent with sensors specifications (i.e., ADXL-355, LIS 3DHH and MPU-6050) or, when not available, with the observations. Importantly, the method adapts to the sensor's characteristics (e.g., sensor noise), allowing to identify the occurrence of relevant events (i.e., presence of signal), without necessarily knowing *a-priori* the sensor specification (noise is calculated with the sensor in-operation). In addition, this method also adapts to changing circumstances, such as "noise" alterations caused by subtle changes in sensor characteristics (resulting from e.g., small displacements or temperature change). When considering a high-density deployment, logistic and maintenance aspects can represent serious bottlenecks unless the system supports adaptive capabilities, as those here described.

4   Deployment and Trials

The MEMS sensor system configured with ADXL355 was deployed in University of Évoras' MITRA site shown in Fig. 4, at a 12 km distance of the city of Évora, that hosts the EVO station, a "Streckeisen STS-2/N" high performance seismometer, that will be used as the reference instrument to compare measurements obtained with the developed MEMS sensor system.
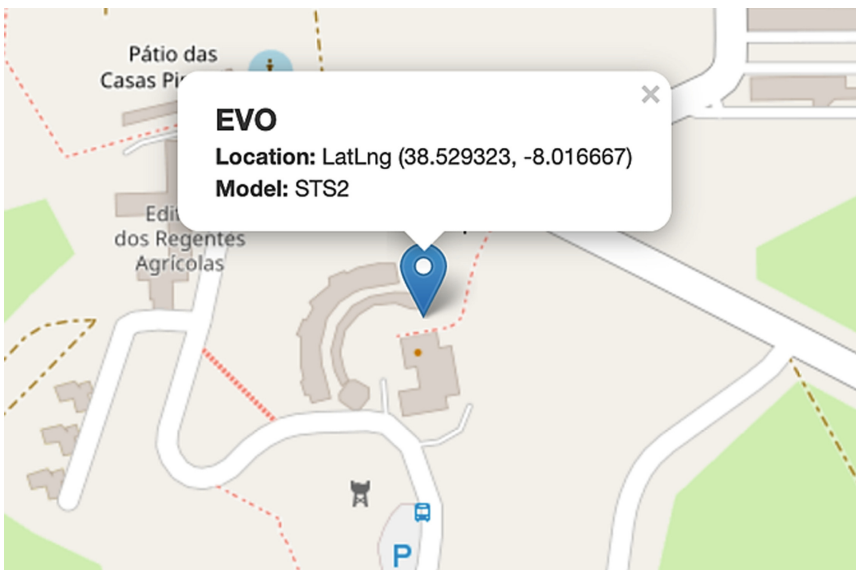

Fig. 4. Location of EVO station at MITRA site.

The MEMS sensor system was installed on 28th July 2020. The sensor is connected to a server hosted by the University of Évora. The sensor sends the measurement readings in real-time to the server using a Wi-Fi Access Point at MITRA.

During the trial phase, it was possible to monitor and detect seismic activity using the developed prototypes, specifically:

a) Event 1: Magnitude 3.4 (ML) with epicentre about 8 km east of Loures (Lisbon district), recorded 18-03-2021 at 9 h 51 (local time) (source: https://www.Ipma.pt/pt/geofisica/comunicados/, accessed 27-March-2021)
b) Event 2: Magnitude 2.5 (ML) with epicentre about 8 km north of Viana do Alentejo (about 10 km from EVO station) recorded 24-March-2021 at 14 h 30 (local time) (source: https://www.ipma.pt/pt/geofisica/comunicados/, accessed 27-March-2021)

4.1   Event 1: Magnitude 3.4 (ML) Recorded 18-March-2021 at 9 h 51 (Local Time)

The Portuguese Institute of the Sea and Atmosphere (IPMA) reported a seismic event with 3.4 magnitude (ML) and epicentre 8 km east of Loures (Lisbon district) that occurred at the 18-March-2021 around 9 h 51 (local time)[2]. The location of the event epicentre, as well as the MEMS sensor system (SSN), is presented in Fig. 5 (source: IPMA website, accessed 27-March-2021).
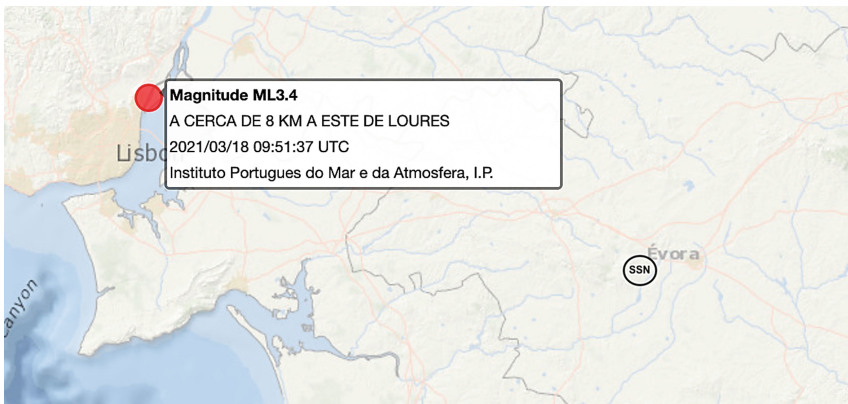

Fig. 5. Location of the seismic event with 3.4 magnitude (ML) with epicentre 8 km east of Loures (Lisbon district) reported by IPMA. The location of the MEMS sensor system is presented in the SSN circle. The MEMS sensor system is located at a distance of about 140 km from the epicentre.

The event was recorded by EVO station, as presented in Fig. 6, showing the arrival of the P-wave close to 9:51:54 (bottom).

---

[2] When the event occurred, Portuguese local time was the same as UTC time.

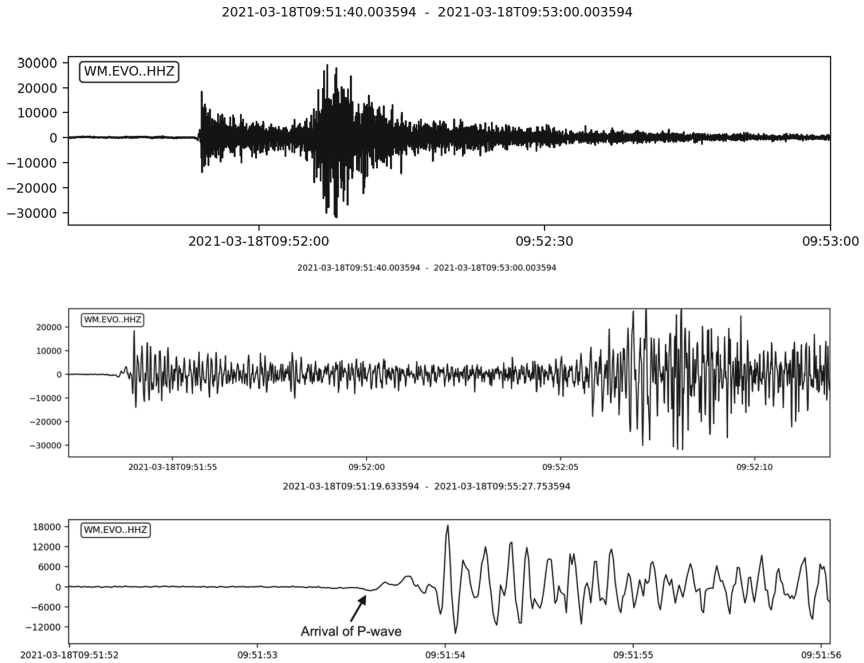2021-03-18T09:51:40.003594 - 2021-03-18T09:53:00.003594

Fig. 6. EVO recording in the Z axis (HHZ) of a 3.4 magnitude event that occurred at March-2021 for a 100 s time window (top), a 60 s time window (middle) and a 4 s window (bottom). The figure's Y-axis shows the raw amplitude value as recorded by EVO. The P-wave is detected close to 9:51:53 (bottom), followed by the start of the S-wave close to 9:52:05. At 9:53:00, EVO still records level of ground activity above what was recorded before the event. [26].
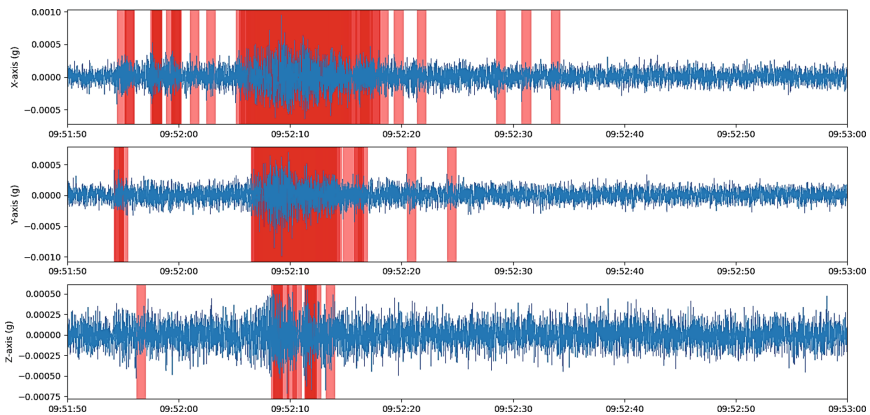

Fig. 7. Overview of acceleration measurements over the three axes for the sensor system over a 70 s time window (9:51:50 and 9:53:20 local time). The X-axis recorded the highest amount of ground motion activity. First detections start at about 9:51:54. The period with strongest activity starts at 9:52:05 continuing until 9:52:15 (the X-axis continues until 9:52:20). In overall, the presence of sensor noise does not allow observing presence of weak signals after 9:52:20 [26]. (Color figure online)

Recorded Signal and Detectability of the MEMS Sensor System

MEMS sensor system recorded data is presented for the time-window of interest of 70 s (9:51:50 and 9:53:30 local time) in Fig. 7. Accelerometer data includes the acceleration value for each of the 3-axis. Acceleration is expressed as a function of *g*. The acceleration offset is removed by subtracting the acceleration mean value over the time window. Detections (likely presence of signal) are colored with background red.

IPMA's reported seismic event with 3.4 magnitude (ML) had an epicentre at a distance of about 140 km from the prototypes. Based on the accelerometer data recorded by the MEMS sensor system, it was shown that a first detection occurred at about the same time (9:51:54) and that it detects the periods of strongest activity.

Spectrogram

A spectrogram analysis is presented for a time window of 20 s. In this analysis, EVO generated spectrograms (using raw measurements), presented in Fig. 8, are used as reference to compare with those generated from the MEMS sensor system, presented in Fig. 9.
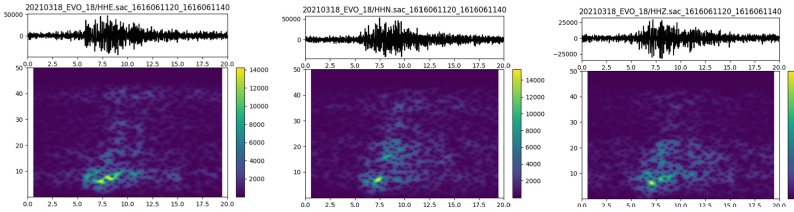

Fig. 8. Spectrograms related with EVO raw measurements for a time window of 20 s. The first column refers to EVO X-axis (HHE), the second column to EVO Y-axis (HHN) and the third column to EVO Z-axis (HHZ). In overall, the recorded signal show predominant frequencies around 10 Hz [26].
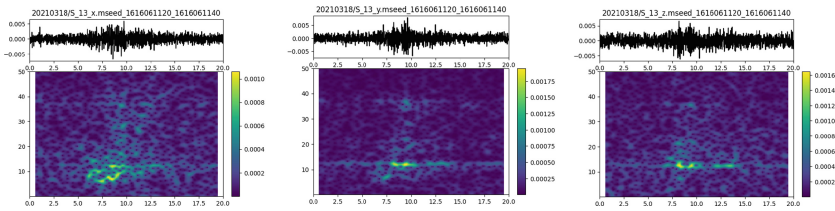

Fig. 9. Spectrograms related with acceleration measurements from the MEMS sensor system for a time window of 20 s (9:52:00 and 9:52:20 local time). The first column refers to the X-axis, the second column to the Y-axis and the third column to the Z-axis. In overall, the recorded signal produces frequency gains predominantly around 10 Hz [26].

In the X-axis, close to the region of maximum signal intensity (10 s), dominant frequencies cluster around 10 Hz (10 Hz is also dominant over time). The high dispersion in signal frequencies indicate presence of noise.

In the Y-axis, close to the region of maximum signal intensity (10 s), the dominant frequency is 10 Hz.

In the Z-axis, close to the region of maximum signal intensity (10 s), the dominant frequencies cluster around 10 Hz (10 Hz is also dominant over time).

The analysis in the frequency domain provides additional insights concerning the observation of the event of interest. The spectrograms generated from EVO raw measurements show that the recorded signal show predominant frequencies around 10 Hz in all X-Y-Z axes. Compared with EVO, the MEMS sensor system exhibit a higher dispersion of signal across several frequencies (being sensor noise a cause), yet there is a dominance of the 10 Hz frequency across all axis.

4.2 Event 2: Magnitude 2.5 (ML) Recorded 24-March-2021 at 14 h 30 (Local Time)

IPMA reported a seismic event with 2.5 magnitude (ML) and epicentre 8 km north-northwest of Viana do Alentejo (Évora district) that occurred at the 24-March-2021 around 14 h 30 (local time)[3]. The location of the event epicentre, as well as the MEMS sensor system (SSN), is presented in Fig. 10 (source: IPMA website, accessed 27-March-2021).
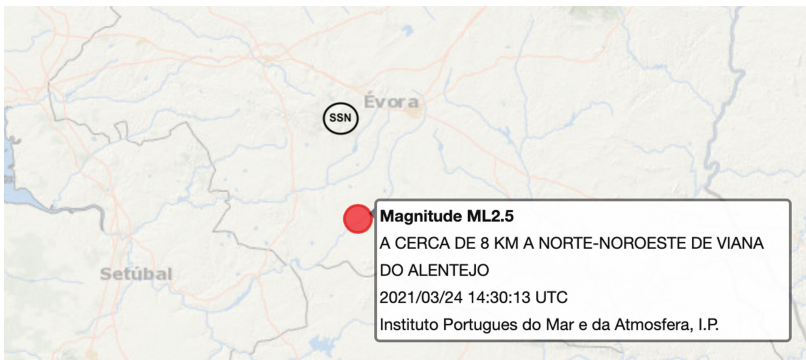

Fig. 10. Location of the seismic event with 2.5 magnitude (ML) with epicentre 8 km north-northwest of Viana do Alentejo (Évora district) reported by IPMA. The location of the MEMS sensor system is presented in the SSN circle. The MEMS sensor system is deployed at a distance of about 10 km from the epicentre.

The event was recorded by EVO station, as presented in Fig. 11, showing the start of the event close to 14:29:39 (bottom) in an increase in ground motion activity after 14:29:41. It is noted that the event time recorded by the EVO station is before IPMA's reported time at 14:30:13. Subsequent analysis concluded that EVO time synchronisation (based on the GPS module) was not operating correctly.

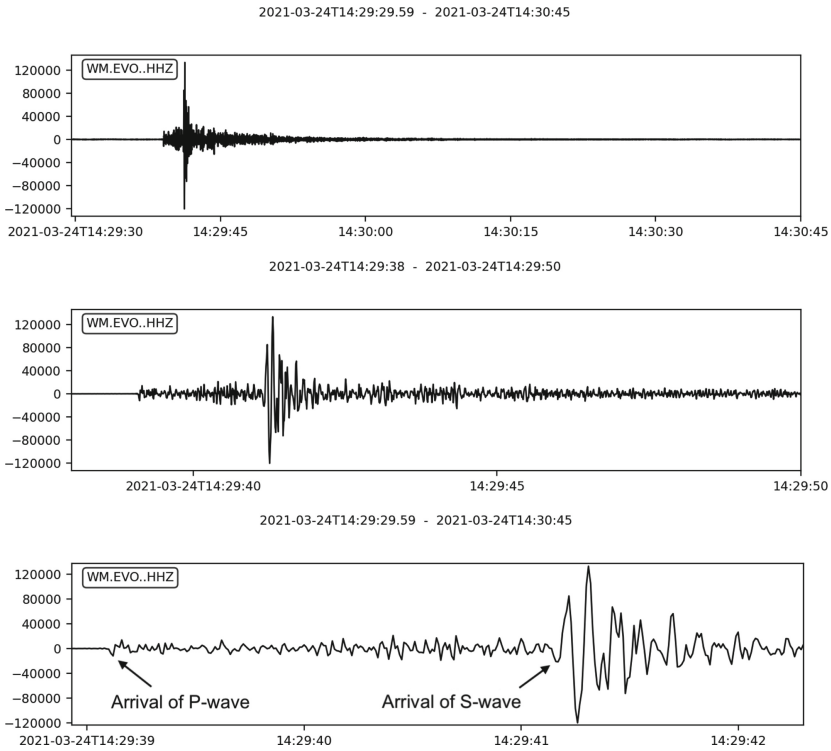[3] When the event occurred, Portuguese local time was the same as UTC time.

Fig. 11. EVO recording in the Z axis (HHZ) of a 2.5 magnitude (ML) for a 45 s window (top), a 12 s time window (middle) and a 3 s window (bottom). The figure's Y-axis shows the raw amplitude value as recorded by EVO. The event starts with the arrival of the P-wave at 14:29:39 (bottom), followed by the S-wave at about 14:29:41. At 14:30:00 (top), EVO still records ground activity above what was present before the event[26].

Recorded Signal and Detectability of the MEMS Sensor System

Recorded accelerometer data is presented for the time-window of interest of 20 s (14:30:15 and 14:30:35 local time). Accelerometer data includes the acceleration value for each of the 3-axis. Acceleration is expressed as a function of *g*. The acceleration offset is removed by subtracting the acceleration mean value over the time window. Detections (likely presence of signal) are colored with background red. It is noted that, since the time window in this subsection differs from the previous one (that used a time window of one hour), detections might differ.

IPMA's reported a seismic event with 2.5 magnitude (ML) had an epicentre at a distance of about 10 km from the prototypes. Based on the accelerometer data recorded by the MEMS sensor system, it was shown that the event was detected after 14:30:15 being active for most of the time window (especially in the X-axis) (Fig. 12).

Observations indicate that the MEMS sensor system is capable to detect the event.

Moreover, it is important to note that the time of the event, as reported by IPMA, is at 14:30:13, while the EVO station identifies first activity occurring at 14:29:39 (with its strong activity recorded between 14:29:41 and 14:29:43). The sensor prototypes report
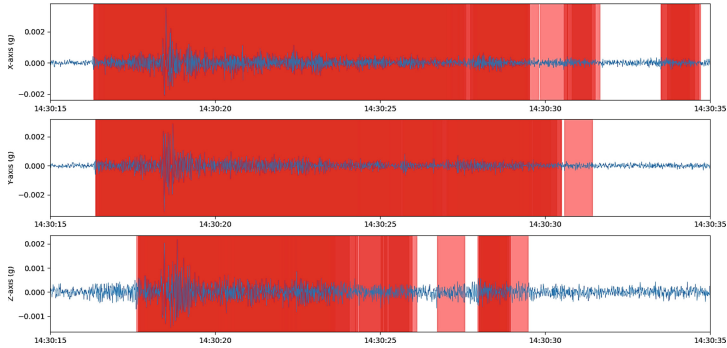
Fig. 12. MEMS sensor system acceleration measurements over a 20 s time window (14:30:15 and 14:30:35 local time). Detections are marked with a 'red' vertical rectangle. The event is detected in all axis after 14:30:16, with strongest amplitude above 2 mg for all axes. The X-axis exhibits the highest acceleration amplitude and detection over time [26]. (Color figure online)

the event as occurring between 14:30:17 and 14:30:25. Given the gap between EVO reported time of the event and IPMA's (that is closer to the sensor prototypes reported time), subsequent analysis concluded that EVO time synchronisation (based on the GPS module) was not operating correctly.

Spectrogram

A spectrogram analysis is presented for a time window for a time window of 15 s. In this analysis, EVO generated spectrograms (using raw measurements), presented in Fig. 13, are used as reference to compare with those generated from the MEMS sensor system, presented in Fig. 14.
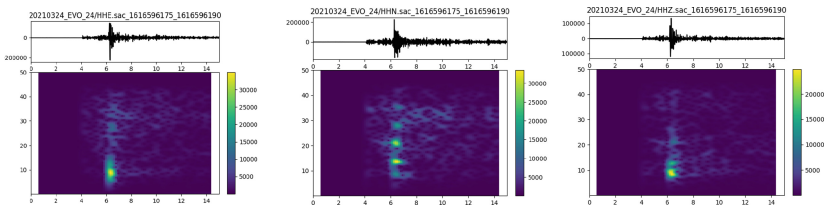

Fig. 13. Spectrograms related with EVO raw measurements for a time window of 15 s. The first column refers to EVO X-axis (HHE), the second column to EVO Y-axis (HHN) and the third column to EVO Z-axis (HHZ). In overall, the recorded signal show predominant frequencies around 10 Hz (in the X and Z EVO axis) and 10 Hz, 20 Hz, 30 Hz and 35 Hz in the Y-axis (EVO HHN) [26].

In the X-axis, close to the region of maximum signal intensity (close to 4 s), dominant frequencies cluster around 10 Hz and spread up to 40 Hz (10 Hz dominates over time). The high dispersion in the presence of frequencies indicate presence of noise. In the Y-axis, close to the region of maximum signal intensity (close to 4 s), dominant frequency is 10 Hz (10 Hz is also dominant over time). In the Z-axis, close to the region of maximum
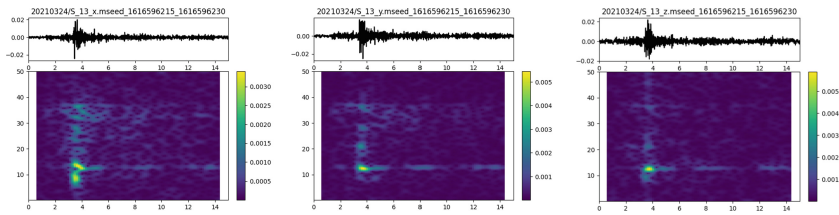
Fig. 14. Spectrograms related with acceleration measurements from the MEMS sensor system for a time window of 15 s (14:30:15 and 14:30:30 local time). The first column refers to the X-axis, the second column to the Y-axis and the third column to the Z-axis. In overall, the recorded signal produces frequency gains predominantly around 10 Hz [26].

signal intensity (close to 4 s), dominant frequency is 10 Hz (10 Hz is also dominant over time).

The spectrograms generated from EVO raw measurements show that the recorded signal show predominant frequencies around 10 Hz in the X and Z EVO axis (HHE and HHZ) and 10 Hz, 20 Hz, 30 Hz and 35 Hz in the Y-axis (HHN). Compared with EVO, the MEMS sensor system exhibit a higher dispersion of signal across several frequencies (being sensor noise a cause) however it is also visible a dominance of the 10 Hz frequency in X-axis and Z-axis, and 10 Hz, 20 Hz, 30 Hz and 35 Hz in the Y-axis (HHN) (for all sensors).

4.3 Findings

In this section, it was presented the results of field trials involving the MEMS sensor system using the ADXL355 sensor. The prototypes were installed in the MITRA site that hosts the EVO station, a "Streckeisen STS-2/N" high performance seismometer. The EVO station was used as reference instrument in comparing and assessing measurements obtained with the developed prototypes.

During this work, two seismic events were monitored and detected using the developed prototypes, specifically: One event of Magnitude 3.4 (ML) with epicentre about 8 km east of Loures (Lisbon district), recorded 18-03-2021 at 9 h 51 (local time) and one event of Magnitude 2.5 (ML) with epicentre about 8 km north of Viana do Alentejo (about 10 km from EVO station) recorded 24-March-2021 at 14 h 30 (local time). These events allowed to demonstrate the sensors capabilities in detecting weak (2.5 ML) to moderate (3.4 ML) events at short (10 km) and medium (140 km) distances, respectively. Comparing with the EVO professional seismometer, however, the sensor prototypes exhibited a higher presence of sensor noise.

5 Conclusion and Future Work

In this chapter it has been addressed the potential for high-density networks for seismic monitoring aiming to improve the resolution of the recorded seismic activity and consequently improving our understanding of the physical processes that cause earthquakes, as well of obtaining more detailed seismic characterisation of studied regions.

It was identified that MEMS technology, used to produce small size accelerometers, has a potential application in seismology. Indeed, MEMS accelerometers have enabled the deployment of high-density seismic networks capable to monitoring seismic activity with high spatial resolution. Example of high-density networks include CalTech's Community Seismic Network (CSN), MyShake Platform and SSN-Alentejo, the latter in deployment phase.

In this context, this chapter described the work conducted to design and deploy low-cost seismic sensor systems, based on low-cost MEMS accelerometers. The sensor system selected for deployment used the ADLX 355 accelerometer. A high-performance seismic station was used as reference sensor for comparison.

During field deployment and evaluation two seismic events were monitored and detected. These events allowed to demonstrate the sensors capabilities in detecting weak to moderate events at short and medium distances.

The following main conclusions can be drawn:

- The architecture herein defined has been demonstrated to be effective in the development and implementation of a MEMS sensor system. The architecture delivers real-time sensor data globally accessible over the Internet.
- Low-cost MEMS accelerometers are effective in detecting strong motion events. From the assessed MEMS accelerometers, the ADXL355 is the best performing, being expected to detect earthquakes with $M = 3$ and $M = 5$ at a distance larger than 10 km and 100 km respectively.
- Low-cost MEMS accelerometers exhibit high levels of self-noise well above Peterson's NHNM, limiting their application in seismology to moderate and strong motion events.
- Low-cost MEMS accelerometers exhibit characteristics that complement seismometers, given their high range and high natural frequency. MEMS accelerometers can be installed next to seismometers, providing additional insights concerning seismic activity and seismology in general.

In order to improve the sensor network capabilities, a few areas for improvement are suggested to be addressed in future work:

- The used low-cost MEMS accelerometers exhibit higher amplitude values and lower damping than those recorded by reference station EVO. Signal processing could be applied to make MEMS measurements closer to EVO.
- The sensor system measurements exhibit bias, which needs to be corrected before they can be used. Techniques for in-field calibration could be developed reducing burden for a large sensor network.
- Time synchronisation needs to be improved, either by using better techniques based on NTP or by incorporating highly accurate time sources like GPS.
- Combine multiple sensors operating as a single logical sensor, improving overall data quality by performing data analytics and correlation and obtain a class-A sensor (comparable to traditional seismometers).

While current MEMS accelerometers performance limits their application in seismology, it is expected that next generation MEMS accelerometers will generate reduced electronic self-noise and will improve frequency response, especially for low frequencies (below Hz), thus capable to compete with traditional seismometers and eventually becoming the *de facto* technology in seismology.

References

1. Rafferty, J.P.: The 6 Deadliest Earthquakes since 1950. Encyclopedia Britannica. https://www.britannica.com/list/6-deadliest-earthquakes. Accessed 2 Oct 2021

2. Ousadou, F., Bezzeghoud, M.: Seismicity of the Algerian tell atlas and the impacts of major earthquakes. In: Bendaoud, A., Hamimi, Z., Hamoudi, M., Djemai, S., Zoheir, B. (eds.) The Geology of the Arab World—An Overview. SG, pp. 401–426. Springer, Cham (2019). https://doi.org/10.1007/978-3-319-96794-3_11

3. Caldeira, B., et al.: Recent improvements in the broadband seismic networks in Portugal. EMSC Newsl. **22**, 18–19 (2007)

4. Carrilho, F., et al.: The Portuguese national seismic network—products and services. Seismol. Res. Lett. **92**(3), 1541–1570 (2021). https://doi.org/10.1785/0220200407

5. Veludo, I., et al.: Crustal seismic structure beneath Portugal and southern Galicia (Western Iberia) and the role of Variscan inheritance. Tectonophysics, 717, 16 October 2017, pp. 645–664 (2017)

6. Custódio, S., et al.: Ambient noise recorded by a dense broadband seismic deployment in Western Iberia. Bull. Seismol. Soc. Am. **104**(6), 2985–3007 (2014). https://doi.org/10.1785/0120140079

7. Palomeras, I., et al.: Finite-frequency Rayleigh wave tomography of the western Mediterranean: mapping its lithospheric structure. Geochem. Geophys. Geosyst. **15**(1), 140–160 (2014)

8. Wachilala, P., Borges, J., Caldeira, B., Matias, L., Rio, I., Bezzeghoud, M.: Characterization of the Region of Arraiolos, South Portugal – Period of January–May 2018. Ass. IUGG 2019, Montreal, Canada (2019)

9. Manso, M., Bezzeghoud, M., Caldeira, B.: Design and evaluation of a high throughput seismic sensor network. tools for planning, deployment and assessment. In: 6th International Conference on Sensor Networks SENSORNETS, Porto, Portugal, 19–21 February (2017)

10. Marco, M., Silva, H., Bezzeghoud, M.: PLASMA - a high-performing and open platform for the integration of heterogeneous sensor networks. In: Fifth Meeting of Post-Graduation in Physics and Earth Sciences of University of Évora, 21–22 September 2011

11. Inbal, A., Clayton, R., Ampuero, J.: Imaging widespread seismicity at midlower crustal depths beneath Long Beach, CA, with a dense seismic array: evidence for a depth-dependent earthquake size distribution. Geophys. Res. Lett. **42**(15), 6314–6323 (2015)

12. Cochran, E., Lawrence, J., Christensen, C., Chung, A.: A novel strong-motion seismic network for community participation in earthquake monitoring. IEEE Instru. Meas. Mag. **12**(6), 8–15 (2009)

13. Anderson, D.P.: BOINC: a system for public-resource computing and storage report. In: 5th IEEE/ACM International Workshop on Grid Computing, Pittsburgh, Pennsylvania, 8 November 2004

14. Clayton, C., Heaton, T., Kohler, M., Chandy, M., Guy, R., Bunn, J.: Community seismic network: a dense array to sense earthquake strong motion. Seismol. Res. Lett. **86**(5), 1354–1363 (2015). https://doi.org/10.1785/0220150094

15. Allen, R.M., Kong, Q., Martin-Short, R.: The myshake platform: a global vision for earthquake early warning. Pure Appl. Geophys. **177**(4), 1699–1712 (2019). https://doi.org/10.1007/s00024-019-02337-7

16. Manso, M., Bezzeghoud, M., Borges, J., Caldeira, B., Abdelhakim, A.: High-density seismic network for monitoring Alentejo region (Portugal) and Mitidja basin region (Algeria). Arab. J. Geosci. **13**(976), 2020 (2020). https://doi.org/10.1007/s12517-020-05972-w

17. Manso, M., Bezzeghoud, M.: On-site sensor noise evaluation and detectability in low cost accelerometers. In: 10th International Conference on Sensor Networks SENSORNETS, Online streaming, 9–10 February 2021

18. Lainé, J., Mougenot, D.: A high-sensitivity MEMS-based accelerometer. Lead. Edge. **33**, 1234–1242 (2014). https://doi.org/10.1190/tle33111234

19. Evans, J., et al.: Performance of several low-cost accelerometers. Seismol. Res. Lett. **85**(1), 147–158 (2014)

20. Farine, M., Thorburn, N., Mougenot, D.: General Application of MEMS Sensors for Land Seismic Acquisition – Is it Time? (2003). http://cseg.ca/assets/files/resources/abstracts/2003/218S0130.pdf

21. Pakhomov, A., Pisano, D., Sicignano, A., Goldburt, T.: Testing of new seismic sensors for footstep detection and other security applications. In: Sensors, and C3I Technologies for Homeland Security and Homeland Defense IV. Proceedings of SPIE, vol. 5778. SPIE, Bellingham, WA (2005) doi: https://doi.org/10.1117/12.604005

22. D'Alessandro, A., Luzio, D., D'Anna, G.: Urban MEMS based seismic network for post-earthquakes rapid disaster assessment. Adv. Geosci. **40**, 1–9 (2014)

23. Scudero, S., D'Alessandro, A., Greco, L., Vitale, G.: MEMS technology in seismology: A short review. In: 2018 IEEE International Conference on Environmental Engineering (EE). 12–14 March 2018. Milan, Italy (2018). https://doi.org/10.1109/EE1.2018.8385252

24. Evans, J., Hamstr, R., Spudich Jr, P., Kündig, C., Camina, P., Rogers, J.: TREMOR: A Wireless, MEMS Accelerograph for Dense Arrays. U.S. Department of the Interior, U.S. Geological Survey. Open-file Report 03–159 (2003)

25. Comunicações Geológicas: Contributor with article Design and Implementation of a Network Enabled High-Throughput MEMs-based Seismic Sensor. Comunicações Geológicas. **103**(1), 107–111 (2016). ISSN: 0873–948X; e-ISSN: 1647–581X

26. Manso, M.: Design and Prototyping of a Network-Enabled Low-Cost Low-Power Seismic Sensor Monitoring System (Doctoral dissertation). Universidade de Évora, Évora, Portugal (2021)